Early stage weathering systematics of Pb and Nd isotopes derived from a high-Alpine Holocene lake sediment record

Finn Süfke[1,2*], Marcus Gutjahr[1], Adrian Gilli[3], Flavio S. Anselmetti[4], Lukas Glur[5], Anton Eisenhauer[1]

[1]GEOMAR Helmholtz-Zentrum für Ozeanforschung Kiel, Wischhofstr. 1–3, 24148 Kiel, Germany

[2]Institute of Earth Sciences, Heidelberg University, Im Neuenheimer Feld 234, Heidelberg, Germany

[3]Geological Institute, ETH Zürich, Zürich, Switzerland

[4]Institute of Geological Sciences and Oeschger Centre for Climate Change Research, University of Bern, Bern, Switzerland

[5]Eawag, Swiss Federal Institute of Aquatic Science and Technology, Dübendorf, Switzerland

*Corresponding author: Finn Süfke, finn.suefke@geow.uni-heidelberg.de

Keywords:

- Lead isotopes
- Neodymium isotopes
- Chemical weathering
- Lake sediment
- Congruent / incongruent weathering

Abstract

Radiogenic Pb and Nd isotopes are well established tools in palaeoceanographic science tracing ambient climate and continental runoff to the oceans down to sub-millennial timescales. Particularly in case of Pb isotopes, a clear climate dependency of continental isotopic runoff on glacial-interglacial transitions has been observed. Pb isotopes were reported to be released incongruently during initial chemical weathering. This incongruent release implies that Pb isotopic runoff compositions differ from the bulk catchment Pb isotopic signal. Yet only little is known about the processes leading to the incongruent release and the timescales of weathering on the continents. In this study we targeted the adsorbed trace metal signature in sediments from a Swiss high-Alpine lake that have accumulated since the retreat of the large Alpine ice domes during the last deglaciation to investigate initial Pb and Nd isotope weathering processes in a granitic environment. Additionally, selected adsorbed element concentrations and ratios were analysed to complement the isotopic physico-chemical weathering information. The integrity of the presented isotope records is supported

by further investigation into the lake environment (e.g. oxic/anoxic conditions) and its potential influence on the isotopic record. The Pb isotope records during the early lake phase witnessed high-amplitude isotopic fluctuations linked to the initial chemical weathering of fine glacial substrate. This finding is also supported by the lithology of the core and rapidly decreasing adsorbed Th and U concentrations. Following this early lake phase, the majority of the Holocene traced congruent release of $^{207}Pb/^{204}Pb$ and $^{206}Pb/^{204}Pb$ and a significant depletion of $^{208}Pb/^{204}Pb$ in the adsorbed phase. These findings corroborate earlier suggestions of more effective weathering of uranogenic minerals yet also call for the presence of more weathering-resistant thorogenic minerals in the lake catchment. The latest 2.2 ka of the record are significantly overprinted by anthropogenic Pb deposition coinciding with the rise and fall of the Roman Empire. Finally, our data suggest that Nd isotopes are equally affected by incongruent weathering during the initial deglacial weathering processes, albeit at smaller magnitude than seen for Pb isotopes.

1. Introduction

Deep marine authigenic Nd and Pb isotope records are increasingly used for paleoceanographic reconstructions aiming to trace weathering fluxes from the continents and overturning dynamics (Reynolds et al., 1999; Foster and Vance, 2006; Gutjahr et al., 2009). The riverine dissolved Nd isotope signal supplied to the oceans is thought to reflect the average isotopic composition of the drainage area (Goldstein and Jacobsen, 1988; Rousseau et al., 2015). Such a situation may not necessarily be the case for the supply of dissolved Pb isotopes to the marine environment, for which the dissolved input can be significantly more radiogenic than the particulate fraction (Crocket et al., 2012; Basak and Martin, 2013). This incongruent release of Pb in the weathering environment (Blanckenburg and Nägler, 2001) has been the focus of various field- and laboratory-based investigations and was ascribed to the preferential weathering of accessory U- and Th-rich mineral phases during early stages of chemical weathering (Erel et al., 1994; Harlavan et al., 1998; Harlavan and Erel, 2002; Dausmann et al. in review).

While the behaviour of Nd during chemical weathering and its transfer to the oceans is well constrained in the modern environment, such investigation of the exogenic Pb isotope distribution in modern times is unfortunately impossible due to human activity. The

anthropogenic atmospheric pollution with Pb led to a remarkable overprint of the natural isotopic signal already since ancient Greek and Roman times (~2.6 ka BP) (e.g. Settle and Patterson, 1980; Bränvall et al., 2001) making it a proxy for tracing human activity instead of natural processes since the invention of larger-scale ore smelting.

To gain a better understanding for the behaviour of Pb isotopic runoff at the regional or local scale during various stages of chemical weathering, other archives than marine records should be tested. Lake sediments are known to record valuable climate information (e.g. Glur et al., 2015; Williams et al., 1997; Melles et al., 2012), yet to date no attempt has been made to extract past dissolved lake Pb or Nd isotopic compositions incorporated into authigenic fractions within their sediments. Although lake sediments deposited within the past ~2.6 ka would very likely be affected by anthropogenic Pb contributions (Renberg et al., 2002), older sediments within the same sediment cores may well have preserved the natural Pb isotopic composition for a given time in the past.

This study aims to constrain Holocene chemical weathering dynamics for Pb and Nd isotopes in a high-Alpine environment by targeting the paleo-lake Pb and Nd isotope composition incorporated into the authigenic fraction of lacustrine sediments. In contrast to marine settings that sample large input sources and bedrock geologies, a high-Alpine lake environment provides ideal boundary contributions since its catchment is very small and the lithology is well constrained. Any temporal changes or trends in isotopic composition of the paleo-lake signature can therefore be attributed to weathering processes/stages alone as opposed to provenance changes. Since Pb isotope runoff compositions are expected to record most exotic (radiogenic) excursions in the transition from pronounced glacial erosion to early stages of chemical weathering (Kurzweil et al., 2010; Crocket et al., 2012), we chose Lake Grimsel in the Swiss Alps in a valley previously occupied by the Rhône ice dome and the Aare Glacier during the preceding Last Glacial Maximum and deglaciation (Kelly et al., 2006). Since our study also extends to the investigation of the extracted adsorbed major and trace elemental concentrations in the authigenic fraction, we are able to constrain both the lake elemental budget besides its Pb and Nd isotopic evolution throughout the Holocene. Sedimentary processes and conditions (e.g. redox conditions) have been investigated to work out a general view on the lake environment and to underline the reliability of the isotope data to represent weathering signals.

2. Sampling site, materials and methods

Sediments used in this study were recovered during sediment coring carried out in winter 2010. Lake Grimsel is a high Alpine lake (>1900 m.a.s.l.) in the central Swiss Alps (Fig.1a). It was dammed in 1929 CE and comprises now a catchment area of nearly 100 km^2. The active Aare Glacier is located within this modern catchment and the bedrock consists of mainly granite with different metamorphic overprints and minor carbonates (Labhart, 1977; Wehrens et al., 2017). Before the damming in 1929 CE lake dimensions and its catchment was quite different. The natural Lake Grimsel (Suppl. Fig A1) was much smaller spanning just a few hundred metres in diameter. It was located in the most eastern part of the modern reservoir lake. During the Holocene the natural lake was not connected to the Aare Glacier and the catchment area was much smaller with 2.8 km^2 (hence less than 3 % of its current size), located between the natural lake and Grimsel Pass (Fig. 1d). The natural catchment area consists almost entirely of the same granitic bedrock, the Grimsel-Granodiorit (Labhart, 1977).

Sediments from a composite sediment core taken from the deepest part of natural Lake Grimsel (Fig. 1c) were analysed for its Pb and Nd isotopic signatures as well as the respective elemental composition in the authigenic sediment phase. Additionally, the Pb and Nd isotope composition of the terrigenous fraction after removal of the adsorbed phase was determined for 18 selected samples. Overall 117 samples have been recovered for analysis of the adsorbed signal spanning the last 10 ka (Holocene) covering the complete lake history and evolution. The age model of the core is based on eight radiocarbon ages retrieved from wood and terrestrial macrofossils (Glur et al., 2013; Wirth et al., 2013b). The composite length of the core is 6.28 m. Sediments are characterized by changing lithologies throughout the Holocene with highest variability in the oldest section (Fig. 2). Grey clayish layers are interbedded with brown organic rich layers in the deepest part (~1m) of the core. The most abundant regular sediment type throughout the Holocene is described as gyttja with a brown appearance (Anselmetti et al., 2007). The gyttja deposits are intercalated mm- to cm-scale clastic layers interpreted as flood layers. In the natural sediment section of Lake Grimsel, 86 such layers can be identified (Wirth et al., 2013b). During sampling for this study these turbiditic layers have been avoided aiming to target only the long-term non-flood sedimentation with its adsorbed elemental and isotopic signal in the lake. The uppermost ~50 cm that were deposited after

127 damming in 1929 CE in a lake hydrologically connected the Aare Glacier catchment, are
128 composed of grey-coloured proglacial varves (Anselmetti et al., 2007).
129 Techniques for the reductive extraction of authigenic Fe-Mn oxyhydroxides are well
130 established for marine sediments (Gutjahr et al., 2007; Blaser et al., 2016) but have not been
131 tested so far on lake sediments. The efficiency of the leaching solutions was tested in a series
132 of three reductive and one oxidising step with increasing reagent concentrations (see
133 supplementary table B.1) in order to identify the most reliable extraction method. Unwanted
134 extraction of Nd or Pb from the lithogenic fraction should lead to isotopic trends in the
135 extracted phase away from the originally adsorbed Nd and Pb isotopic signature (cf. Blaser et
136 al., 2016). Before reductive leaching, the sediments were always first rinsed with deionised
137 water (18.2 MΩ, MQ grade) followed by ~0.5M $MgCl_2$ for the removal of lightly adsorbed Pb
138 (i.e., potentially acquired contaminant Pb during sediment storage in repository). The $MgCl_2$
139 was removed afterwards by triple rinses with deionised water followed by centrifugation and
140 decanting (MQ). As a first active extraction step we applied the dilute reductive leaching
141 solution as used in Blaser et al. (2016) in two consecutive leaching steps for 30 minutes in a
142 shaker. The supernatant was collected each time via pipetting after centrifugation (10 min at
143 4000 rpm). Following the second extraction, the same sediment was treated with the tenfold
144 more concentrated leaching solution as originally presented in Gutjahr et al. (2007) for one
145 hour, followed by centrifugation and collection of the supernatant. After the reductive
146 leaching steps, a relatively aggressive oxidizing 4.5M HNO_3 solution was used aiming to
147 provoke the partial dissolution of the lithogenic phase alongside the adsorbed fraction. The
148 results (Fig. 3) show no noticeable changes in the Pb isotopic composition for the first three
149 gentle reductive leaching steps while the Nd isotopic composition of the first leachate fraction
150 is gradually less radiogenic than the two subsequent ones. For most elements highest
151 concentrations (normalised to the mass of sediment used) were observed during the first of
152 the three reductive extraction steps, while overall highest concentrations were achieved
153 during strong acid leaching (Suppl. Fig. A2). Given the reproducible extraction of an authigenic
154 Pb isotopic signature over the three successive reductive leaching steps, the adsorbed signal
155 of all 117 sediment samples was subsequently extracted using 20 ml of the reductive leaching
156 solution of Blaser et al. (2016) for 1 hour on 500 to 700 mg of wet sediment. The leaching
157 solution used consisted of 1.5% acetic acid, 0.005 M hydroxylamine hydrochloride, 0.003M
158 Na-EDTA buffered to pH ~4 with 0.35M NaOH. Prior to total dissolution of selected samples

the previously reductively leached sediment samples have been exposed to the leaching solution of Gutjahr et al. (2007) for a further 24 hours to remove any remaining Fe-Mn oxyhydroxides. Afterwards samples were centrifuged and the supernatant decanted. Sediments have been dried, ground and ~50 mg of dry sediment weighed out in PFA vials for total digestion. Organic material was first removed in three steps using 2 ml of conc. HNO_3 on a hotplate, followed by exposure to 1ml conc. HNO_3 and 1 ml of 30% H_2O_2 at room temperature for one night and finally using 2 ml of aqua regia on a hot plate for one night. Subsequently, the remaining sediments were digested with conc. HF-HNO_3-HCl in a microwave. Fluorides forming after the microwave digestion in hydrofluoric acid were taken care of via three evaporation steps in concentrated HNO_3 before elemental separation. Pb and Nd fractions for isotopic analyses were purified using standard techniques (Lugmair & Galer, 1992; Cohen et al., 1988). Total procedural Pb blanks were below 18 pg, while Nd procedural blanks were below 70 pg for the adsorbed fraction and 0.2 ng for the detrital fraction. In both cases the contribution to the measured signal was below 0.1 % and hence insignificant.

Pb and Nd isotope compositions were measured with a Thermo Scientific Neptune Plus MC-ICP-MS at GEOMAR Kiel. Machine-induced mass-bias for Nd was corrected for internally using the approach of Vance and Thirlwall (2002). Mass-bias corrected results were normalised to accepted $^{143}Nd/^{144}Nd$ of 0.512115 (Tanaka et al., 2000). Secondary in-house standards "SPEX" reproduced at 0.511085 ± 5 (2 SD, n=7) and NIST 3135a at a $^{143}Nd/^{144}Nd$ of 0.512452 ± 7 (2 SD, n=13; all Nd solutions measured at 50 ppb). Note that NIST3135a standard is only certified for its Nd concentration, not its isotopic composition. $^{143}Nd/^{144}Nd$ isotopic compositions of samples are given as εNd by normalisation to the Chondrite Uniform Reservoir ($^{143}Nd/^{144}Nd_{CHUR}$= 0.512630; Bouvier et al., 2008). Mass-bias correction for Pb (measured at 28 ppb Pb) was carried out by doping all samples and standards with a 7 ppb Tl standard solution (Walder and Furuta, 1993;Belshaw et al., 1998) yet aiming for a Pb/Tl of ~4. In contrast to these pioneering studies, we adjusted the NIST 997 Tl standard $^{205}Tl/^{203}Tl$ on a session-by-session basis so that the sum of all offsets of the average mass bias corrected NIST SRM 981 Pb isotope ratios matched published compositions of Baker et al. (2004). Given that six isotope pairs of Pb exist minute offsets to the literature NIST SRM 981 remain (on the order of few ppm) yet this methods accounts for the fact that all six Pb isotope ratios are measured statically in the same sample solution and hence the sum of isotopic offsets compared with

191 the original Baker et al. (2004) data should be zero ppm (see Suppl. Table A8). Using this
192 approach the slightly different ionisation behaviour of Tl in plasma mass spectrometry
193 compared with Pb is accounted for as known from earlier studies (cf. Thirlwall, 2002)). A large
194 batch of reductively leached USGS NOD-A-1 ferromanganese nodule standard powder
195 measured throughout the course of this project reproduced at $^{206}Pb/^{204}Pb$ = 18.964 (± 0.002),
196 $^{207}Pb/^{204}Pb$ = 15.685 (± 0.003), $^{208}Pb/^{204}Pb$ = 38.956 (± 0.008), $^{208}Pb/^{206}Pb$ = 2.0542 (± 0.0002)
197 and $^{207}Pb/^{206}Pb$ = 0.8271 (± 0.0001) (all uncertainties are 2 SD, n=22) after normalisation to
198 the NIST SRM 981 compositions reported in Baker et al. (2004) (Suppl. Table A8).
199 Finally, elemental concentrations for Pb, Sr, Ti, Ca, Fe, Mg, Li, Nd, Al, Th, U and Mn of aliquots
200 from the leaching step have been determined using an Agilent Series 7500 ICP-MS at GEOMAR
201 Kiel. All isotopic and elemental data are listed in the Suppl. Tables A2-A8. All results will also
202 be accessible on the Pangea database (www.pangaea.de).

203

204 ## 3. Results

205 Elemental observations

206 Based on extracted adsorbed elemental concentrations three major phases within the
207 Holocene can be defined (Fig. 4). The first phase, reflecting relatively early deglacial conditions
208 after retreat of the Aare Glacier, spans the earliest ~1000 years of the record. Highest Th and
209 U yields were recovered from this section with steeply decreasing concentrations during the
210 early Holocene (note that all concentrations are shown as ng/g or μg/g of leached sediment).
211 In contrast, lowest extractable adsorbed Al and Ti concentrations were found in the oldest
212 part and highest concentrations in the mid- and late Holocene. Generally, highest short-term
213 variability in elemental concentrations with most extreme short-term fluctuations is observed
214 during the oldest interval. The second phase spans the period from ~9 ka BP until the year
215 1929 (i.e., the damming of the lake). It is characterized by low Th and U concentrations while
216 [Al] remains high. Pb concentrations are elevated and most variable in the oldest part of the
217 record, decreasing slightly towards the middle of the Holocene with an increasing trend in the
218 last ~1000 years attributable to anthropogenic activity (see section 4.6 below). The third phase
219 covers the interval after the year 1929 reflecting entirely changed hydrologic conditions after
220 the damming of the lake. Elements such as Al and Fe show a sharp, distinct decrease in
221 concentrations in this youngest part of the record while the concentrations of other elements

sharply increase, mirroring trends seen in the oldest part of the lake record. Mn is only enriched in the uppermost part of the sediment. Elemental ratios (Al/Nd, Al/Th and Mn/Fe; Fig. 4) delineate the same pattern than observed for the respective elemental concentrations. Trends in Mn/Fe originate from another process than weathering during the Mid-Holocene and will be discussed separately (see section 4.2).

Pb and Nd isotopic trends

The various Pb isotopic trends and compositions ($^{206}Pb/^{204}Pb$, $^{207}Pb/^{204}Pb$, $^{208}Pb/^{204}Pb$, $^{207}Pb/^{206}Pb$ and $^{208}Pb/^{206}Pb$) of the adsorbed signal as well as that of the detrital signal are presented in Fig. 5. Figure 6 further illustrates selected Pb isotope ratios alongside the extracted Pb, Th and U concentrations for the natural part of the Lake Grimsel Pb isotope record. In the adsorbed Pb isotopic signal, also three phases can be identified, which differ in time from these seen before due to different processes affecting the isotopic signal. The first phase is dominated by short-term fluctuations in the isotopic composition as seen before but ends nearly 500 years earlier (~9.6 ka BP; Fig. 5) than seen for elemental concentrations. This phase is dominated by a radiogenic excursion at the beginning of the record for $^{206}Pb/^{204}Pb$, $^{207}Pb/^{204}Pb$ and $^{208}Pb/^{204}Pb$ and correspondingly low $^{207}Pb/^{206}Pb$ and $^{208}Pb/^{206}Pb$ ratios. Despite small isotopic excursions the natural part (9.6-2.2 ka BP) of the Holocene Pb isotopic composition is remarkably invariant compared with the earliest part of the record, only defining a muted secular trend over the natural Holocene part of the Pb isotope record (Fig. 6 a,c,e). The beginning of anthropogenic Pb deposition after 2.2 ka BP is clearly recognizable (Fig. 5). At 1.2 ka BP a brief return to almost natural Holocene Pb isotopic values is observable. Most strikingly $^{206}Pb/^{204}Pb$ and $^{207}Pb/^{206}Pb$ for almost all depths for which both the adsorbed and terrigenous signal was determined are either more or less identical or possibly slightly more radiogenic in the adsorbed phase. In contrast $^{208}Pb/^{204}Pb$ in the adsorbed fraction is depleted compared with the terrigenous signal. The isotopic compositions seen in the detrital fraction are more variable than those in the adsorbed phase. We attribute this to the relatively small sample size (<0.8 g per sample) that resulted in partially non-representative isotopic information regarding the whole-rock composition (Buchter et al., 1994). Besides, the Pb isotopic composition of the adsorbed and detrital phase in the most recent 1200 years follow the same anthropogenically perturbed trend, suggesting incomplete removal of the adsorbed phase in the sediments prior to total digestion of the residue.

Nd isotope signatures for the adsorbed and the detrital signal are relatively radiogenic for a granitic setting with an average ε_{Nd} value of -4.04 ± 0.8 (2 SD) for all detrital Nd isotope compositions apart from the youngest data point (Fig. 5). While the detrital ε_{Nd} scatter around a mean composition, the adsorbed signal follows a settle trend towards less radiogenic ε_{Nd} throughout the Holocene, yet always displaying more radiogenic ε_{Nd} than the corresponding terrigenous fraction. Distinct temporal phases as observed for the Pb isotopic records are less pronounced. The Nd isotopic offset between adsorbed and terrigenous signal becomes smaller towards the latest Holocene. The unradiogenic isotope excursion in the most recent sample (1970 CE) is controlled by the significantly enlarged and distinct modern catchment area and direct connection with the glacial catchment of the Aare Glacier after the damming of the lake.

4. Discussion

The key aim of our study is an assessment towards the possibility to reconstruct the Lake Grimsel dissolved trace metal evolution throughout the Holocene. To this end, we first need to consider whether an unbiased extraction of the adsorbed phase can be carried out, which phase is actually targeted during reductive leaching, and whether redox-controlled processes may have been compromising an originally incorporated Nd and Pb isotope signature downcore. The physico-chemical weathering information contained in the various isotopic and elemental records is discussed after a positive verdict is reached regarding the integrity of the records.

4.1. Origin and type of the authigenic phase (adsorbed signal)

The mild reductive leaching method (Blaser et al., 2016) adapted from marine sediments is supposed to target authigenic Fe-Mn oxyhydroxides hosting the adsorbed trace metal signal. In Lake Grimsel, it is, however, unclear whether oxyhydroxides formed during the Holocene lake evolution (i) have been present throughout, (ii) whether evidence can be provided for postdepositional remobilization of Fe-Mn oxyhydroxides, and (iii) what type of authigenic phase may have been present and dissolved instead. Bottom- and/or sediment pore water oxygenation of Lake Grimsel throughout its evolution has not been studied to date and redox

conditions might have prevented the formation and/or preservation of authigenic Fe-Mn oxyhydroxides during the Mid-Holocene (Davison, 1993; see section 4.2). The Pb and Nd isotopic signal extracted during gentle reductive sequential leaching is fairly robust (Fig. 3). Even repeated gentle reductive extraction steps on sedimentary aliquots recovered the same Pb isotope signal that is usually not identical to compositions if a more aggressive (4.5M HNO_3) solution was used that is expected to also attack the terrigenous fraction in the sediment. Despite this positive result an assessment should be made whether the recovered signal corresponds to the originally adsorbed Lake Grimsel composition. If various elemental and isotopic records are extracted in unaltered originally adsorbed concentrations (Figs. 4-6), this would point towards the extraction of an authigenic phase other than Fe-Mn oxyhydroxides. We also note in this context that Boyle (2001) has shown that Pb will only migrate in redox sediments under very low sedimentation rates (below 10 cm/ka), hence conditions, which are not given here.

It is possible that organic matter, equally complexing or incorporating major and trace elements in the lake, may effectively scavenge dissolved ions under sub/anoxic conditions. El Bilali et al. (2002) have shown that concentrations of certain elements, including Pb, are positively correlated with organic carbon concentrations. Furthermore, the evidently smoother evolution of the adsorbed Nd and Pb isotope signal compared with the terrigenous signal is likely a function of the averaging effect of slow trace metal precipitation on possibly decadal or centennial timescales from lake water. Such a feature, however, may also hint at diagenetic remobilisation (smoothing) of an originally incorporated more variable adsorbed Pb isotope signature. None of the elemental (Fig. 4) and Pb isotopic data (Figs. 5, 6) suggest the presence of such diagenetic fronts with the exception of a Mn concentration maximum in the topmost 108 cm, corresponding to the past ~900 years of lake evolution. The Nd isotope record does not appear as clearly pristine and despite its lower sampling density we cannot dismiss the possibility of some post burial diagenetic smoothing of the original Nd isotopic signal. On the other hand, the normalised extracted Nd concentrations do not suggest diagenetic remobilisation since normalised concentrations display small-scale variability as seen for other elements such as Al (Fig. 4). Particularly the occasional short-term variability in the extracted authigenic Pb isotope records argues for the preservation of an originally dissolved lake Pb isotope signal. The most clear-cut example for this process is the very sharp appearance of anthropogenically sourced Pb in the lake record at 2.2 ka BP (Figs. 5 and 8; see

316 section 4.6). Overall we are fairly confident that the extracted authigenic trace metal signal of
317 the lake sediments was preserved independent from the O_2 concentration of the bottom
318 water with potential question marks for the Nd isotope record and the Mn and Fe
319 concentrations under low-oxygen conditions (see section 4.2). This in turn suggests that either
320 (i) redox conditions did not lead to bottom-/porewater anoxia (regarded unlikely, see section
321 4.2), (ii) diagenetic dissolution of Fe-Mn oxyhydroxides in the sediment did only mobilise
322 redox-sensitive elements such as Mn or Fe, or (iii) trace metals chemically extracted in this
323 study were associated with a redox-insensitive phase such as organic ligands (Tessier et al.,
324 1985).

325

326 ## 4.2. Redox influence on isotopic/elemental records

327 Alpine lakes are known to become sub-/anoxic either permanently (e.g. Wirth et al., 2013a)
328 or seasonally caused for example by ice cover in winter and the formation of a stratified water
329 column. In case of Lake Grimsel the adsorbed Mn concentrations during the early lake phase
330 (10-9 ka BP, Fig. 4) equally shows an enrichment in extractable Mn to that observed in XRF
331 core scanning bulk sediment records (Wirth et al. 2013a) (Fig. 4). During an early, distinct
332 transition phase from oxic to anoxic conditions the Mn signal is variable and becomes stable
333 and depleted within the majority of the Holocene when bottom water anoxic conditions were
334 established. Recurrent enrichments in Mn concentrations within the Holocene may be the
335 result of short-time ventilation caused by mass movement events (Wirth et al., 2013a).

336 In section 4.1 it was concluded that the Pb isotope evolution, potentially the Nd isotope
337 record, as well as the large majority of elemental records appear to record originally
338 incorporated adsorbed trace metal contents and isotopic compositions. The clearly resolvable
339 onset of the anthropogenic excursion in the Lake Grimsel Pb isotope record (see section 4.6)
340 is the most obvious proof for this suggestion. Uranium is another redox-sensitive trace metal
341 that may help assessing elemental mobility (e.g. Tribovillard et al., 2006). During anoxic
342 conditions U precipitate in sediments as UO_2 from reduction of more soluble uranium (VI)
343 carbonate complexes (Langmuir, 1978; Klinkhammer and Palmer, 1991) and becomes
344 enriched while it is highly soluble in oxygenated waters (e.g. Tribovillard et al., 2006). Our
345 normalised U concentration record (Fig. 4) displays no obvious indication for redox-dependent
346 U mobility. However, our analytical approach is most likely incapable of targeting potentially

present sedimentary uraninite since a gentle reducing solution was employed to extract the authigenic signal. It is unlikely that such a reagent targeted uraninite present in the sediment because of its stability against dissolution (e.g. Parks and Pohl, 1988). Observations made in the presented lake record suggest a different behaviour of U. Both during the earliest and most recent lake phase U is enriched in the adsorbed phase of the sediment (Fig. 4). Mn only shows high concentrations in the uppermost part tracing Mn mobilisation in the sediment (Lynn and Bonatti, 1965). The observation that U is much more closely related to the concentration pattern to Th, which is not influenced by redox conditions (Bonatti et al., 1971), and not Mn suggests that the lower- and uppermost U concentration peaks display elevated weathering input rather than local redox conditions (see section 4.3.)

On the other hand, elements like Fe and Mn are known to be strongly redox sensitive (Schaller et al., 1997) and a diffusive exchange within the sediment cannot that easily be excluded. Then again, diagenetic fronts should be visible but can only be identified in the Mn record (see section 4.1).

Although it appears that some of the originally present Mn was probably lost via diagenetic remobilisation we test the Fe/Mn record for its redox sensitivity and an estimation of the redox conditions during sedimentation. Several studies (Naeher et al., 2013; Wersin et al., 1991; Lopez et al., 2006; Koinig et al., 2003) suggested that the Mn/Fe ratio can be used as a redox proxy for lacustrine sediments due to the dependency of the sedimentary Mn/Fe ratio to the formation and dissolution of Fe- and Mn-oxids under different oxygenation conditions. The ratio is highest in the earliest lake phase during the transition phase seen during the earliest Holocene and in the latest part of the record when conditions were oxic (Fig. 4). During the majority of the Holocene the ratio is lower than 0.01 indicating permanent anoxic bottom water conditions (Koinig et al., 2003). We note that adsorbed Mn concentrations reported here are not directly comparable to bulk sediment concentrations since Mn is dominantly supplied from the authigenic fraction in Lake Grimsel sediment, adding some uncertainty to the comparability of the earlier study and the current. During phases with lowest ratios in the order of 0.001 (7.9 – 6.8, 6.0 – 5.7, 4.3 – 3.65, 3.45 – 2.8, 2.0 – 0.9 ka BP; Fig. 3) most element concentrations are decreased. Some elements (e.g. Al) are more affected than others (e.g. Nd, Th, Ti) as seen in Al/(Nd, Th) minima during these bottom water conditions. The observation that these low Mn/Fe intervals are not capped with elemental concentration spikes for any displayed element (Fig. 4) suggests generally reduced elemental fluxes into the sediments

during these low-oxygen intervals as opposed to diagenetic migration of trace metals within the pore waters with continuing sedimentation.

4.3. Local deglaciation and physico-chemical weathering trends

For the understanding of the presented results, in particular for the adsorbed Pb isotope signal, it is essential to take a closer look at the chronology of glacier retreat and incipient lake sedimentation. Kelly et al. (2006) have reconstructed the deglaciation history of the Grimsel Pass region by dating the surface exposure with ^{10}Be ages. For the Grimsel Pass, an ice-free-age of 11.3 ka BP was presented, predating our record by nearly 1000 years. On the other hand, various assumptions have to be made in ^{10}Be surface exposure dating like the complete removal of previously present ^{10}Be by glaciers and errors on the order of 1000 years are likely. Moreover, Lake Grimsel is located ~300 m below the Grimsel Pass in an area covered by the Aare Glacier even after the retreat of the Rhône ice dome freed the Grimsel Pass. Consequently, Lake Grimsel might have been covered by ice well after 11.3 ka BP. Given these uncertainties our record may have recorded last stages of the deglaciation of the Lake Grimsel area.

The Pb isotopic weathering signal after initial glacier retreat will vary as a function of weathering stage. Rock substrate previously exposed to dominantly physical (peri-)glacial erosion is subsequently exposed to chemical weathering reactions in the Lake Grimsel catchment. The first released Pb isotope signal during incipient chemical weathering is expected to be congruent, implying that the dissolved lake signature should correspond to the average particulate input signal. This congruency is controlled by Pb contributions from reactive surfaces of all rock-forming minerals exposed to weathering as opposed to dominating Pb release from U-/Th-rich accessory mineral phases (e.g. sphene, apatite; Dausmann et al., in review) which represent up to 2-5 % of the mineral content in the Grimsel-Granodiorite (Stalder, 1964). The subsequent runoff will slowly evolve towards more radiogenic ^{206}Pb/^{204}Pb due to preferential radiogenic Pb release from uranogenic trace mineral phases such as apatite (Erel et al. 1994; Harlavan et al., 1998). Harlavan et al. (1998) also reported the preferential release of ^{208}Pb alongside ^{206}Pb and ^{207}Pb. Such preferential release of the ^{232}Th daughter could not be confirmed by Dausmann et al. (in review), who observed rather the opposite of ^{208}Pb retention during early chemical weathering since most

thorogenic minerals appeared to be more weathering resistant in their study. This striking isotopic difference is likely a function of the presence/absence of certain Th-rich accessory mineralogy phases (e.g. sphene) in the catchment. The relative importance of uranogenic and thorogenic minerals during chemical weathering is also reflected in the runoff $^{208}Pb/^{206}Pb$ when compared to bulk source rock compositions.

Normalised adsorbed U and Th concentrations in our record decreased early during the lake evolution in less than a few hundred years after beginning sedimentation (Fig. 6). Such a sharp significant reduction of dissolved U, Th and to a lesser extent Pb input into Lake Grimsel resembles plagioclase reaction rates presented by White and Brantley (2003). These authors attributed the parabolic decrease of reaction rates to the duration of exposure of chemical weathering including factors such as (i) intrinsic surface area increase, (ii) progressive depletion of energetically reactive surfaces and (iii) accumulation of leached layers and secondary accumulates. The early Holocene reduction of dissolved U and Th fluxes into Lake Grimsel sediments does not coincide with a significant change in $^{206}Pb/^{204}Pb$, $^{208}Pb/^{204}Pb$ or $^{208}Pb/^{206}Pb$ (Fig. 6). Our data therefore suggests that the reduction in dissolved trace metal input is not a function of already depleted U- and Th-rich accessory mineral phases but instead controlled by reduced weathering rates with increasing duration of chemical weathering. In other words: while overall cationic input into the lake was decreasing during the earliest lake evolution, accessory U- and Th-rich mineral phases were still present in the catchment and continued to contribute to the dissolved Pb isotopic input.

All radiogenic Pb isotope ratios become more radiogenic at the onset of lacustrine sedimentation (Figs. 5, 6). Yet, while $^{206}Pb/^{204}Pb$ and $^{207}Pb/^{204}Pb$ are isotopically close to the terrigenous signal suggesting almost congruent release, $^{208}Pb/^{204}Pb$ is depleted (Fig. 5). While the Holocene $^{206}Pb/^{204}Pb$ evolution appears to define a subtle concave-upward isotopic trend throughout most of the natural Pb isotope record (Fig. 6a), such a behaviour is not evident in $^{208}Pb/^{204}Pb$ (Fig. 6c).

In the following we compare our Holocene Pb isotopic trends to results of various weathering studies dedicated to Pb isotope systematics (Erel et al., 1994; Harlavan & Erel, 2002; Harlavan et al., 2009) as well as studies focusing on the elemental release during granitoid weathering (Middelburg et al., 1988; Harriss & Adams, 1966). Harlavan et al. (2009) found timespans of 140-300 ka before the weathering of accessory minerals becomes negligible beneath the

441 weathering of aluminosilicates, hence significantly longer than monitored here (~10.5 ka).
442 Middelburg et al. (1988) have shown that Th for example is immobile during the first stage of
443 chemical weathering, a suggestion in agreement with observations made in our study and by
444 Dausmann et al. (in review). The late deglacial radiogenic Pb isotope excursion, the sharply
445 decreasing Th and U concentrations as well as the unstable signal seen in all presented records
446 (isotopic and elemental) can therefore most realistically be ascribed to the efficient
447 weathering of fine rock substrate/powder during incipient chemical weathering conditions. It
448 is likely that ongoing physical erosion below the retreating glacier in the catchment during the
449 earliest Lake Grimsel evolution generated fine rock substrate/powder (Anderson, 2007).
450 Under efficient physical glacial erosion of rock substrate (i.e. effectively creating rock
451 powders), all radiogenic Pb isotopes will be released congruently since even the more
452 weathering-resistant Th-rich accessory mineral phases will contribute to the runoff Pb isotope
453 signal (Dausmann et al., in review).

454 The purpose of selecting Alpine Lake Grimsel for this physico-chemical weathering study was
455 to monitor the Pb isotopic weathering behaviour in a well-constrained and spatially limited
456 granitic catchment. The lithological input into the lake did overall not change significantly in
457 terms of source-rock composition. Conversely, presence or absence of (peri-)glacial physical
458 weathering is expected to affect the elemental and isotopic lake water evolution. It is
459 conceivable that the variability of the grain size distribution in the catchment could have
460 influenced the adsorbed signal for some adsorbed elements. The resemblance of the earliest
461 sediments (greyish clays) with recent sediments (after damming of the lake) (Fig. 2) is
462 noteworthy and therefore can indeed be interpreted as sub-/proglacial rock powder, while
463 sediments throughout the Holocene contained much higher organic carbon contents and no
464 glacially generated sediment. In addition, most elements show the same pattern in their
465 concentrations for the most recent sediments after the damming of the lake and in the earliest
466 lake phase (Fig. 4). Today the lake and the sediments are clearly influenced by glacial processes
467 within the active Aare Glacier catchment. Since elemental concentrations particularly of Al, U
468 and Th are very comparable to earliest deglacial trends we suggest that processes seen today
469 (active glacial erosion) can similarly be applied to the earliest lake phase. For obvious reasons
470 this comparison cannot be carried out for modern Pb isotopic trends (see section 4.6).

471

4.4. Incongruent weathering of Nd

Earlier studies (e.g. Frank, 2002; Van De Flierdt et al., 2002) have insinuated the incongruent weathering of Nd isotopes and the potential implications on the Nd budget in the oceans. Indeed the incongruent release of Nd isotopes was reported during weathering of boreal tills (Öhlander et al., 2000; Andersson et al., 2001) and exposure of stream sediments from Greenland to mild leaching reagents during laboratory-based chemical weathering experiments (Blanckenburg and Nägler, 2001). Recent experimental work by Dausmann et al. (in review) demonstrated that the incongruent release of radiogenic Nd from accessory minerals occur during very early stages of chemical weathering. The presented Nd isotope record from Lake Grimsel could either reflect leaching artefacts such as observed during too vigorous leaching of marine sediments (e.g. Elmore et al., 2011), or indeed reliably trace the dissolved Lake Grimsel Nd isotope signature adsorbed in lake sediments. We cannot entirely disprove the possibility for the existence of preferential release of Nd from certain accessory phases during leaching as opposed to chemical weathering releasing such an incongruent signature to the lake. The chemical extraction approach used here is identical to that used in Blaser et al. (2016) for deep North Atlantic sediments, and these authors recovered reliable bottom water ε_{Nd} even at challenging sediment core sites around Iceland. Additionally, more aggressive leaching tests performed within the context of our study (section 2 above) have shown that partial dissolution of a detrital phase would cause an increase in the Nd concentration which is more than one order of magnitude higher than concentrations observed in the Holocene adsorbed record (Suppl. Fig. A2). Furthermore, adsorbed Nd concentrations and Nd isotope excursions show no correlation within the Holocene (Suppl. Fig. A3). Partial dissolution of a detrital mineral phase causing the radiogenic offset seems therefore very unlikely. Even in the unlikely case that our extracted Nd isotope record was controlled by preferential dissolution of accessory mineral phases during chemical extraction, the generally decreasing offset between terrigenous and extracted ε_{Nd} signatures throughout the Holocene (Fig. 5) calls for the presence of incongruent release of Nd during early chemical weathering.

Despite its lower temporal resolution compared with the presented Pb isotope records (Fig. 5), the ε_{Nd} record illustrates the distinct behaviour of Nd compared with Pb in an aqueous environment. Nd is less particle-reactive and therefore short-term variations as seen in the Pb isotope records are less pronounced or absent due to the longer residence time in water

(Frank, 2002). The slightly more radiogenic adsorbed ε_{Nd} signal and its secular trend towards the terrigenous signature is interpreted to present a lake water composition and therefore weathering input signal. It is hence likely that Nd isotopes display incongruent weathering behaviour during the first thousands of years of chemical weathering in a granitic catchment such as observed here. The net effect on the ocean Nd budget is likely negligible due to the relative small offset (~1 ε_{Nd} unit) between adsorbed and detrital signal.

4.5. Lack of immediate climate sensitivity of the Pb and Nd isotope signals

Results presented so far focused on the longer-term Holocene Pb and Nd isotopic evolution of the chemical weathering input into Lake Grimsel without consideration of short-term climate extremes. While physico-chemical weathering rates will vary as a function of climate and intensity of the hydrologic cycle (Kump et al., 2000), authigenic records in Alpine lakes may not necessarily record climate excursions of short duration. A comparison of our Pb isotope data with a climate record derived from Milchbach speleothems (9.2 – 2.0 ka BP) located near Grindelwald (Luetscher et al., 2011) show no tight coupling (Fig. 7). Both regional and transregional climate data display just a weak or no clear correlation with all presented records. Even the Misox event (8.2 – 8.0 ka BP), the strongest cold event within the Holocene, cannot be resolved either in the isotopic or elemental records. This lack of correlation suggests that early high Alpine weathering mechanisms are linked to internal factors within the Holocene. For example, the early Holocene (post-deglacial phase) was strongly influenced by the supply and dissolution of fine rock powder and during the Mid-Holocene anoxic conditions partly control the element pattern. Last but not least, the signal incorporated in the adsorbed signal will also average climatic conditions over decades if not centuries, before the sediment is buried deep enough not to chemically interact anymore with lake conditions above. Neither the adsorbed Pb nor the Nd isotope records traced centennial-scale climate variability, yet this finding is not surprising given that the timescales of physico-chemical weathering are likely an order of magnitude longer than such shorter-term climatic trends (cf. Harlavan et al., 2009).

4.6. Anthropogenic overprint/activity

After 2.2 ka BP the Pb isotopic records underwent the most dramatic and abrupt change in its isotopic composition. The isotopic excursions are significantly more pronounced than during the earliest part of the record. It is very unlikely that these late Holocene excursions are caused by natural perturbations (Settle and Patterson 1980; Renberg et al., 1994; Shotyk et al., 1998). From modern ocean records we know that the natural Pb signal can easily be overprinted by human activities not only by riverine input but also through the atmosphere by dust and aerosols (Alleman et al., 1999; Schaule and Patterson, 1981). Settle & Patterson (1980) have summarized the anthropogenic world Pb production of the last 5 ka and detailed the most important milestones in mining and usage of lead ores. It is remarkable that the last 2.2 ka of their lead pollution curve perfectly matches excursions in the presented isotopic record (Fig. 8). The substantial change in the isotopic record at 2.2 ka BP neatly matches the rise of the Roman Empire and their mining activity all over Europe (especially on the Iberian Peninsula; e.g. Grögler et al., 1966) as well as the results of Bränvall et al. (2001) who have shown a change in the isotopic compositions of lake sediments from Sweden at the same time period. At this point only 60% of the adsorbed Pb isotope signal is from a natural source (Suppl. Fig. A4). With the exhaustion of the Roman mines, the fall of the Roman Empire and the cultural perturbations of the medieval times (reduced mining activity) the Pb isotopic signal nearly returned to natural compositions. At 1.2 ka BP 90% of the adsorbed Pb isotope signal was naturally sourced (Suppl. Fig. A4). A similar observation was made by Bränvall et al. (2001). After 1.2 ka the atmospheric, anthropogenic Pb pollution increases exponentially with the accelerating development of the human culture. Beginning with the silver production in Germany, the discovery of America and mining activities there and finally the industrial revolution our $^{206}Pb/^{204}Pb$ isotope record shows the overall most unradiogenic compositions. The resemblance of the presented Pb isotope records with those from Sweden (Bränvall et al., 2001) and the global lead production curve (Settle and Patterson, 1980) we argue that the anthropogenic, atmospheric lead input into Lake Grimsel during the last 2.2 ka years are from a more distant source (e.g. Iberian Peninsula; Grögler et al., 1966) rather than from a regional Alpine source. No (lead) mine has been reported of the Lake Grimsel area from ancient times until today, one reason for choosing this lake for the reconstruction of natural Pb isotope systematics.

Anthropogenic lead introduced in the atmosphere by smelting can precipitated after transport as aerosol particles distant to the place of production (e.g. Renberg et al., 1994; Hong et al.,

1994). These particles may also overprint the natural Pb isotopic signal as observed in the recent 2.2 ka of the presented record (Fig. 8). The two youngest detrital Pb isotope compositions after 1.2 ka BP shown in Fig. 5 are shifted towards an anthropogenic signal. But these results illustrate the none-quantitative removal of adsorbed trace metals with our leaching method than a dominance of atmospheric introduced lead particles. Otherwise Pb isotopic records produced by a much stronger chemical treatment (e.g. Bränvall et al., 2001) should not be comparable to our record.

5. Conclusions

The aim of this study was the extraction of the adsorbed Pb and Nd isotope signatures from Holocene Alpine lake sediments using a gentle reducing and complexing leaching technique that is normally used for marine sediments. Results have shown that isotopic and elemental signatures gained from lake sediments are not only very reliable but also valuable archives for lacustrine physico-chemical weathering reconstructions. The combined investigation of the adsorbed and detrital Pb isotopic composition throughout the Holocene provided valuable insights into the initial deglacial chemical weathering processes in a granitic catchment. The Pb isotope signatures are highly variable during the first hundreds of years of the record, linked to incipient chemical weathering reactions of glacially eroded rock substrate. The remainder of the natural Holocene Pb isotope record is remarkably invariant and only defines a settle secular trend. $^{206}Pb/^{204}Pb$ and $^{207}Pb/^{204}Pb$ of the adsorbed and detrital phase show no noticeable differences indicating congruent release of the uranogenic daughters. On the other hand, $^{208}Pb/^{204}Pb$ is depleted in the adsorbed phase suggesting retention of the thorogenic daughter during the first thousands of years of chemical weathering after glacier retreat. Pb isotopes are known to be released from labile accessory minerals during early stages of chemical weathering yet the observed isotope records indicate congruent release of uranogenic minerals (releasing $^{207}Pb/^{204}Pb$ and $^{206}Pb/^{204}Pb$) alongside other major rock-forming mineral phases. Equally, adsorbed $^{208}Pb/^{204}Pb$ underline the weathering resistance of thorogenic minerals. Analysis of other adsorbed element concentrations and ratios revealed that the lake environment (e.g. oxic/anoxic conditions) and sub-millennial climate perturbations had no noticeable impact on the isotopic weathering signal. This implies that mineral reaction rates in the catchment are either too slow to leave a traceable short-term

climate signal in the adsorbed Pb isotope signature or that the contact time of sediment porewater Pb with overlying lake water is too long, effectively averaging out short-term climate signals. Further we have presented field evidence that even Nd isotopes are likely influenced by incongruent release during initial weathering processes. Throughout the Holocene the offset between adsorbed and detrital phase systematically decreased.

Besides tracing the natural Holocene Lake Grimsel Pb isotope evolution, our record revealed massive Pb isotopic excursions caused by atmospheric anthropogenic Pb deposition. The first excursion in our Pb isotope record matches well with the rise of the Roman Empire after 2.2 ka BP. The second excursion in in our Pb isotope record mimics the onset and evolution of large scale in central Europe and the industrial revolution. Overall this study underlines the potential of lake sediments for weathering studies and for the investigation of anthropogenic influence since ancient times.

Acknowledgements

We thank Ana Kolevica for the support with element analyses and assistance in the laboratory. Furthermore, the work of Florian Kirsch is acknowledged who was a valuable help during sample purification. Huang Huang was always supportive during laboratory work. We thank the Emmy-Noether-Programm of the German Research Foundation (DFG) Grant Li1815/4. Constructive comments by three anonymous reviewers and the editor Catherine Chauvel improved an earlier version of the manuscript and are acknowledged.

References

Alley, R. B., 2004. GISP2 Ice Core Temperature and Accumulation Data. IGBP PAGES/World Data Center for Paleoclimatology. Data Contribution Series #2004-013. NOAA/NGDC Paleoclimatology Program, Boulder Co, USA.

Alleman, L.Y., Véron, A.J., Church, T.M., Flegal, A.R., Hamelin, B., 1999. Invasion of the abyssal North Atlantic by modern anthropogenic lead. Geophys. Res. Lett. 26, 1477–1480. doi:10.1029/1999GL900287

Anderson, S.P., 2007. Biogeochemistry of Glacial Landscape Systems. Annu. Rev. Earth Planet. Sci. 35, 375–399. doi:10.1146/annurev.earth.35.031306.140033

Andersson, P.S., Dahlqvist, R., Ingri, J., Gustafsson, Ö., 2001. The isotopic composition of Nd

627 in a boreal river: A reflection of selective weathering and colloidal transport. Geochim.
628 Cosmochim. Acta 65, 521–527. doi:10.1016/S0016-7037(00)00535-4

629 Anselmetti, F.S., Bühler, R., Finger, D., Girardclos, S., Lancini, A., Rellstab, C., Sturm, M., 2007.
630 Effects of Alpine hydropower dams on particle transport and lacustrine sedimentation.
631 Aquat. Sci. 69, 179–198. doi:10.1007/s00027-007-0875-4

632 Baker, J., Peate, D., Waight, T., Meyzen, C., 2004. Pb isotopic analysis of standards and
633 samples using a 207Pb-204Pb double spike and thallium to correct for mass bias with a
634 double-focusing MC-ICP-MS. Chem. Geol. 211, 275–303.
635 doi:10.1016/j.chemgeo.2004.06.030

636 Basak, C., Martin, E.E., 2013. Antarctic weathering and carbonate compensation at the
637 Eocene–Oligocene transition. Nat. Geosci. 6, 121–124. doi:10.1038/ngeo1707

638 Belshaw, N.., Freedman, P.., O'Nions, R.., Frank, M., Guo, Y., 1998. A new variable dispersion
639 double-focusing plasma mass spectrometer with performance illustrated for Pb
640 isotopes. Int. J. Mass Spectrom. 181, 51–58. doi:10.1016/S1387-3806(98)14150-7

641 Blanckenburg, F., Nägler, T., 2001. Weathering versus circulation controlled changes in
642 radiogenic isotope tracer composition of the Labrador Sea and North Atlantic Deep
643 Water. Paleoceanography 16, 424–434. doi:10.1029/2000PA000550.

644 Blaser, P., Lippold, J., Gutjahr, M., Frank, N., Link, J.M., Frank, M., 2016. Extracting
645 foraminiferal seawater Nd isotope signatures from bulk deep sea sediment by chemical
646 leaching. Chem. Geol. 439, 189–204. doi:10.1016/j.chemgeo.2016.06.024

647 Bonatti, E., Fisher, D.E., Joensuu, O., Rydell, H.S., 1971. Postdepositional mobility of some
648 transition elements, phosphorus, uranium and thorium in deep sea sediments.
649 Geochim. Cosmochim. Acta 35, 189–201. doi:10.1016/0016-7037(71)90057-3

650 Bouvier, A., Vervoort, J.D., Patchett, P.J., 2008. The Lu-Hf and Sm-Nd isotopic composition of
651 CHUR: Constraints from unequilibrated chondrites and implications for the bulk
652 composition of terrestrial planets. Earth Planet. Sci. Lett. 273, 48–57.
653 doi:10.1016/j.epsl.2008.06.010

654 Boyle, J., 2001. Redox remobilization and the heavy metal record in lake sediments: A
655 modelling approach. J. Paleolimnol. 26, 423–431. doi:10.1023/A:1012785525239

656 Bränvall, M.L., Bindler, R., Emteryd, O., Renberg, I., 2001. Four thousand years of
657 atmospheric lead pollution in northern Europe: A summary from Swedish lake
658 sediments. J. Paleolimnol. 25, 421–435. doi:10.1023/A:1011186100081

659 Buchter, B., Hinz, C., Flühler, H., 1994. Sample size determination of a coarse fragment
660 conteny in a stony soil. Geoderma 63, 265–275. doi:10.1016/0016-7061(94)90068-X.

661 Cohen, A.S., O'Nions, R.K., Siegenthaler, R., Griffin, W.L., 1988. Chronology of the pressure-
662 temperature history recorded by a granulite terrain. Contrib. to Mineral. Petrol. 98,
663 303–311. doi:10.1007/BF00375181

664 Crocket, K.C., Vance, D., Foster, G.L., Richards, D.A., Tranter, M., 2012. Continental
665 weathering fluxes during the last glacial/interglacial cycle: Insights from the marine
666 sedimentary Pb isotope record at Orphan Knoll, NW Atlantic. Quat. Sci. Rev. 38, 89–99.
667 doi:10.1016/j.quascirev.2012.02.004

668 Dausmann, V., Gutjahr, M., Frank, M., Kouzmanov, K., Schaltegger, U., in review.
669 Esperimental evidence for mineral-controlled release of radiogenic Nd, Hf, and Pb
670 isotopes from granitic rocks during progressive chemical weathering. Submitted to
671 Chemical Geology

672 Davison, W., 1993. Iron and manganese in lakes. Earth-Science Rev. 34, 119–163.
673 doi:10.1016/0012-8252(93)90029-7.

674 El Bilali, L., Rasmussen, P.E., Hall, G.E.M., Fortin, D., 2002. Role of sediment composition in
675 trace metal distribution in lake sediments. Appl. Geochemistry 17, 1171–1181.
676 doi:10.1016/S0883-2927(01)00132-9

677 Elmore, A.C., Piotrowski, A.M., Wright, J.D., Scrivner, A.E., 2011. Testing the extraction of
678 past seawater Nd isotopic composition from North Atlantic deep sea sediments and
679 foraminifera. Geochemistry, Geophys. Geosystems 12. doi:10.1029/2011GC003741

680 Erel, Y., Harlavan, Y., Blum, J.D., 1994. Lead isotope systematics of granitoid weathering.
681 Geochim. Cosmochim. Acta 58, 5299–5306. doi:10.1016/0016-7037(94)90313-1

682 Foster, G.L., Vance, D., 2006. Negligible glacial-interglacial variation in continental chemical
683 weathering rates. Nature 444, 918–921. doi:10.1038/nature05365

684 Frank, M., 2002. Radiogenic isotopes: Tracers of past ocean circulation and erosional input.
685 Rev. Geophys. 40, 1001. doi:10.1029/2000RG000094

686 Glur, L., Stalder, N.F., Wirth, S.B., Gilli, A., Anselmetti, F.S., 2015. Alpine lacustrine varved
687 record reveals summer temperature as main control of glacier fluctuations over the
688 past 2250 years. Holocene 25, 280–287. doi:10.1177/0959683614557572

689 Glur, L., Wirth, S.B., Büntgen, U., Gilli, A., Haug, G.H., Schär, C., Beer, J., Anselmetti, F.S.,
690 2013. Frequent floods in the European Alps coincide with cooler periods of the past
691 2500 years. Sci. Rep. 3, 1–5. doi:10.1038/srep02770

692 Goldstein, S.J., Jacobsen, S.B., 1988. Rare earth elements in river waters. Earth Planet. Sci.
693 Lett. 89, 35–47. doi:10.1016/0012-821X(88)90031-3

694 Grögler, N., Geiss, J., Grünenfelder, M., Houtermans, F.G., 1966. Isotopenuntersuchungen
695 zur Bestimmung der Herkunft r??mischer Bleirohre und Bleibarren. Zeitschrift fur
696 Naturforsch. - Sect. A J. Phys. Sci. 21, 1167–1172. doi:10.1515/zna-1966-0744

697 Gutjahr, M., Frank, M., Halliday, A.N., Keigwin, L.D., 2009. Retreat of the Laurentide ice sheet
698 tracked by the isotopic composition of Pb in western North Atlantic seawater during
699 termination 1. Earth Planet. Sci. Lett. 286, 546–555. doi:10.1016/j.epsl.2009.07.020

700 Gutjahr, M., Frank, M., Stirling, C.H., Klemm, V., van de Flierdt, T., Halliday, A.N., 2007.
701 Reliable extraction of a deepwater trace metal isotope signal from Fe-Mn oxyhydroxide
702 coatings of marine sediments. Chem. Geol. 242, 351–370.
703 doi:10.1016/j.chemgeo.2007.03.021

704 Harlavan, Y., Erel, Y., 2002. The release of Pb and REE from granitoids by the dissolution of
705 accessory phases. Geochim. Cosmochim. Acta 66, 837–848. doi:10.1016/S0016-
706 7037(01)00806-7

707 Harlavan, Y., Erel, Y., Blum, J.D., 2009. The coupled release of REE and Pb to the soil labile
708 pool with time by weathering of accessory phases, Wind River Mountains, WY.

709 Geochim. Cosmochim. Acta 73, 320–336. doi:10.1016/j.gca.2008.11.002

710 Harlavan, Y., Erel, Y., Blum, J.D., 1998. Systematic Changes in Lead Isotopic Composition with
711 Soil Age in Glacial Granitic Terrains. Geochim. Cosmochim. Acta 62, 33–46.
712 doi:10.1016/S0016-7037(97)00328-1

713 Harriss, R.C., Adams, J.A.S., 1966. Geochemical and mineralogical studies on the weathering
714 of granitic rocks. Am. J. Sci. doi:10.2475/ajs.264.2.146

715 Hong, S., Candelone, J.P., Patterson, C.C., Boutron, C.F., 1994. Greenland ice evidence of
716 hemispheric lead pollution two millenia ago by Greek and Roman civilisations. Science
717 (80-.). 265, 1841–1843. doi:10.1126/science.265.5180.1841.

718 Kelly, M.A., Ivy-Ochs, S., Kubik, P.W., Von Blanckenburg, F., Schlüchter, C., 2006. Chronology
719 of deglaciation based on ^{10}Be dates of glacial erosional features in the Grimsel Pass
720 region, central Swiss Alps. Boreas 35, 634–643. doi:10.1111/j.1502-
721 3885.2006.tb01169.x

722 Klinkhammer, G.P., Palmer, M.R., 1991. Uranium in the oceans: Where it goes and why.
723 Geochim. Cosmochim. Acta 55, 1799–1806. doi:10.1016/0016-7037(91)90024-Y

724 Koinig, K., Shotyk, W., Lotter, a, Ohlendorf, C., 2003. 9000 Years of Geochemical Evolution of
725 Lithogenic Major and Trace Elements in the Sediment of an …. J. Paleolimnol. 4, 307–
726 320. doi:10.1023/a:1026080712312

727 Kump, L.R., Brantley, S.L., Arthur, M.A., 2000. Chemical Weatehring, Atmospheric CO2, and
728 Climate. Annu. Rev. Earth Planet. Sci. 28, 611–667.

729 Kurzweil, F., Gutjahr, M., Vance, D., Keigwin, L., 2010. Authigenic Pb isotopes from the
730 Laurentian Fan: Changes in chemical weathering and patterns of North American
731 freshwater runoff during the last deglaciation. Earth Planet. Sci. Lett. 299, 458–465.
732 doi:10.1016/j.epsl.2010.09.031

733 Langmuir, D., 1978. Uranium solution-mineral equilibria at low temperatures with
734 applications to sedimentary ore deposits. Geochim. Cosmochim. Acta 42, 547–569.
735 doi:10.1016/0016-7037(78)90001-7

736 Lopez, P., Navarro, E., Marce, R., Ordoñez, J., Caputo, L., Armengol, J., 2006. Elemental ratios
737 in sediments as indicators of ecological processes in Spanish reservoirs. Limnetica 25,
738 499–512. doi:10.1144/GSL.SP.2006.267.01.06

739 Luetscher, M., Hoffmann, D.L., Frisia, S., Spötl, C., 2011. Holocene glacier history from alpine
740 speleothems, Milchbach cave, Switzerland. Earth Planet. Sci. Lett. 302, 95–106.
741 doi:10.1016/j.epsl.2010.11.042

742 Lugmair, G.W., Galer, S.J.G., 1992. Age and isotopic relationships among the angrites Lewis
743 Cliff 86010 and Angra dos Reis. Geochim. Cosmochim. Acta 56, 1673–1694.
744 doi:10.1016/0016-7037(92)90234-A

745 Lynn, D.C., Bonatti, E., 1965. Mobility of manganese in diagenesis of deep-sea sediments.
746 Mar. Geol. 3, 457–474. doi:10.1016/0025-3227(65)90046-0

747 Melles, M., Brigham-Grette, J., Minyuk, P.S., Nowaczyk, N.R., Wennrich, V., DeConto, R.M.,
748 Anderson, P.M., Andreev, A.A., Coletti, A., Cook, T.L., Haltia-Hovi, E., Kukkonen, M.,
749 Lozhkin, A. V., Rosén, P., Tarasov, P., Vogel, H., Wagner, B., 2012. 2.8 Million years of

arctic climate change from Lake El'gygytgyn, NE Russia. Science (80-.). 337, 315–320. doi:10.1126/science.1222135

Middelburg, J.J., Van Der Weijden, C.H., Woittiez, J.R.W., 1988. Chemical processes affecting the mobility of major, minor and trace elements during weathering of granitic rocks. Chem. Geol. 68, 253–273. doi:10.1016/0009-2541(88)90025-3

Naeher, S., Gilli, A., North, R.P., Hamann, Y., Schubert, C.J., 2013. Tracing bottom water oxygenation with sedimentary Mn/Fe ratios in Lake Zurich, Switzerland. Chem. Geol. 352, 125–133. doi:10.1016/j.chemgeo.2013.06.006

Öhlander, B., Ingri, J., Land, M., Schöberg, H., 2000. Change of Sm-Nd isotope composition during weathering of till. Geochim. Cosmochim. Acta 64, 813–820. doi:10.1016/S0016-7037(99)00365-8

Parks, G.A., Pohl, D.C., 1988. Hydrothermal solubility of uraninite. Geochim. Cosmochim. Acta 52, 863–875. doi:10.1016/0016-7037(88)90357-2

Renberg, I., Brännvall, M.L., Bindler, R., Emteryd, O., 2002. Stable lead isotopes and lake sediments - A useful combination for the study of atmospheric lead pollution history. Sci. Total Environ. 292, 45–54. doi:10.1016/S0048-9697(02)00032-3

Renberg, T., Persson, M.W., Emteryd, O., 1994. Pre-industrial atmospheric lead contamination detected in Swedish lake sediments. Lett. to Nat. 372, 323–326. doi:10.1038/368323a0

Reynolds, B.C., Frank, M., O'Nions, R.K., 1999. Nd- and Pb-isotope time series from Atlantic ferromanganese crusts: Implications for changes in provenance and paleocirculation over the last 8 Myr. Earth Planet. Sci. Lett. 173, 381–396. doi:10.1016/S0012-821X(99)00243-5

Rousseau, T.C.C., Sonke, J.E., Chmeleff, J., Van Beek, P., Souhaut, M., Boaventura, G., Seyler, P., Jeandel, C., 2015. Rapid neodymium release to marine waters from lithogenic sediments in the Amazon estuary. Nat. Commun. 6. doi:10.1038/ncomms8592

Schaller, T., Moor, H.C., Wehrli, B., 1997. Sedimentary profiles of Fe, Mn, V, Cr, As and Mo as indicator of benthic redox conditons in Baldeggersee. Aquat. Sci. 59, 345–361. doi:10.1007/BF02522363.

Schaule, B.K., Patterson, C.C., 1981. Lead concentrations in the northeast Pacific: evidence for global anthropogenic perturbations. Earth Planet. Sci. Lett. 54, 97–116. doi:10.1016/0012-821X(81)90072-8

Settle, D.M., Patterson, C.C., 1980. Lead in albacore: guide to lead pollution in Americans. Science 207, 1167–76. doi:10.1126/science.6986654

Shotyk, W., Appleby, P.G., Cheburkin, A.K., Frei, R., Gloor, M., Kramers, J.D., Reese, S., Knaap, W.O. Van Der, 1998. History of atmospheric lead depostion since 12,37014C yr BP from a Peat bog, Jura Mountains, Switzerland. Science (80-.). 281, 1635–1640. doi:10.1126/science.281.5383.1635.

Stalder, H.A., 1964. Petrographische und mineralogische Untersuchungen im Grimselgebiet (Mittleres Aarmassiv). Schweizerische Mineral. und Petrogr. Mitteilungen = Bull. Suisse Mineral. Petrogr. 44, 188–384. doi: 10.5169/seals-34334

Tanaka, T., Togashi, S., Kamioka, H., Amakawa, H., Kagami, H., Hamamoto, T., Yuhara, M., Orihashi, Y., Yoneda, S., Shimizu, H., Kunimaru, T., Takahashi, K., Yanagi, T., Nakano, T., Fujimaki, H., Shinjo, R., Asahara, Y., Tanimizu, M., Dragusanu, C., 2000. JNdi-1: A neodymium isotopic reference in consistency with LaJolla neodymium. Chem. Geol. 168, 279–281. doi:10.1016/S0009-2541(00)00198-4

Tessier, A., Rapin, F., Carignan, R., 1985. Trace metals in oxic lake sediments: possible adsorption onto iron oxyhydroxides. Geochim. Cosmochim. Acta 49, 183–194. doi:10.1016/0016-7037(85)90203-0

Thirlwall, M.F., 2002. Multicollector ICP-MS analysis of Pb isotopes using a 207pb-204pb double spike demonstrates up to 400 ppm/amu systematic errors in TI-normalization. Chem. Geol. 184, 255–279. doi:10.1016/S0009-2541(01)00365-5

Tribovillard, N., Algeo, T.J., Lyons, T., Riboulleau, A., 2006. Trace metals as paleoredox and paleoproductivity proxies: An update. Chem. Geol. 232, 12–32. doi:10.1016/j.chemgeo.2006.02.012

Van De Flierdt, T., Frank, M., Lee, D.C., Halliday, A.N., 2002. Glacial weathering and the hafnium isotope composition of seawater. Earth Planet. Sci. Lett. 201, 639–647. doi:10.1016/S0012-821X(02)00731-8

Vance, D., Thirlwall, M., 2002. An assessment of mass discrimination in MC-ICPMS using Nd isotopes. Chem. Geol. 185, 227–240. doi:10.1016/S0009-2541(01)00402-8

Walder, A.J., Furuta, N., 1993. High-Precision Lead Isotope Ratio Measurement by Inductively Coupled Plasma Multiple Collector Mass Spectrometry. Anal. Sci. 9, 675–680. doi:10.2116/analsci.9.675

Wehrens, P., Baumberger, R., Berger, A., Herwegh, M., 2017. How is strain localized in a meta-granitoid, mid-crustal basement section? Spatial distribution of deformation in the central Aar massif (Switzerland). J. Struct. Geol. 94, 47–67. doi:10.1016/j.jsg.2016.11.004

Wersin, P., Höhener, P., Giovanoli, R., Stumm, W., 1991. Early diagenetic influences on iron transformations in a freshwater lake sediment. Chem. Geol. 90, 233–252. doi:10.1016/0009-2541(91)90102-W

White, A.F., Brantley, S.L., 2003. The effect of time on the weathering of silicate minerals: Why do weathering rates differ in the laboratory and field? Chem. Geol. 202, 479–506. doi:10.1016/j.chemgeo.2003.03.001

Williams, D.F., Peck, J., Karabanov, E.B., Prokopenko, A.A., Kravchinsky, V., King, J., Kuzmin, M.I., 1997. Lake Baikal record of continental climate response to orbital insolation during the past 5 million years. Science (80-.). 278, 1114–1117. doi:10.1126/science.278.5340.1114

Wirth, S.B., Gilli, A., Niemann, H., Dahl, T.W., Ravasi, D., Sax, N., Hamann, Y., Peduzzi, R., Peduzzi, S., Tonolla, M., Lehmann, M.F., Anselmetti, F.S., 2013a. Combining sedimentological, trace metal (Mn, Mo) and molecular evidence for reconstructing past water-column redox conditions: The example of meromictic Lake Cadagno (Swiss Alps). Geochim. Cosmochim. Acta 120, 220–238. doi:10.1016/j.gca.2013.06.017

Wirth, S.B., Glur, L., Gilli, A., Anselmetti, F.S., 2013b. Holocene flood frequency across the

Central Alps - solar forcing and evidence for variations in North Atlantic atmospheric circulation. Quat. Sci. Rev. 80, 112–128. doi:10.1016/j.quascirev.2013.09.002

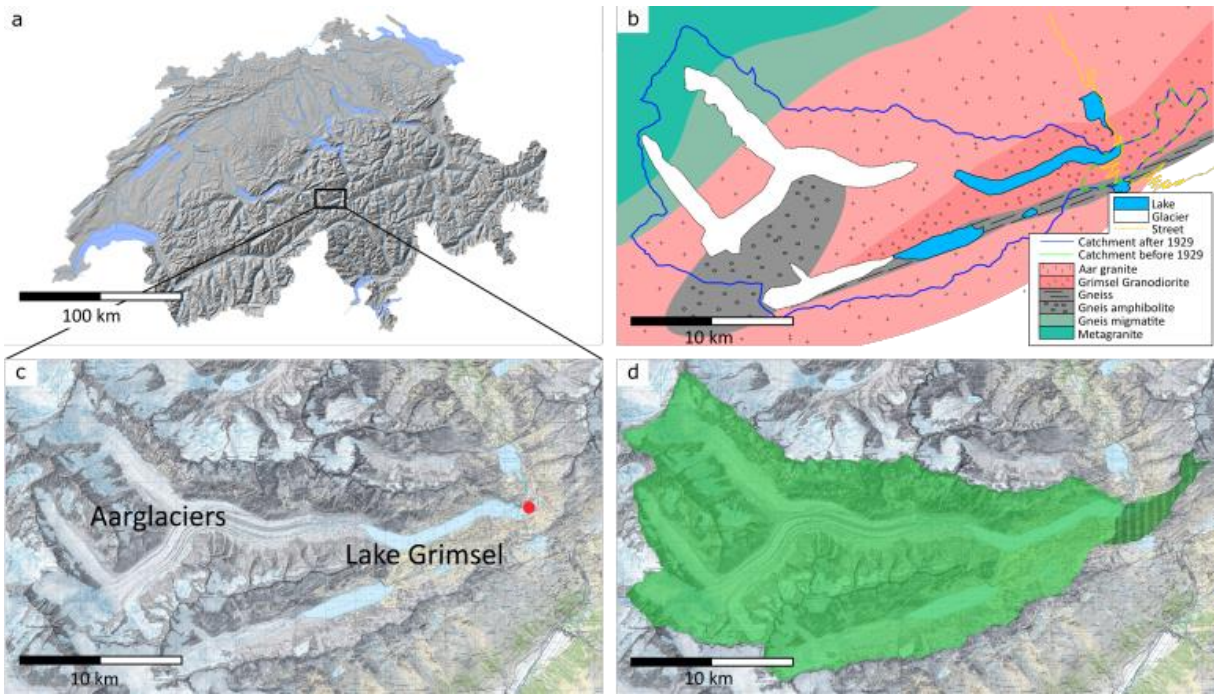

Figure 1: (a) Overview map of Switzerland with the main lake and river systems. (b) simplified geological map of the Lake Grimsel area (based on Stalder, 1964; Abrecht, 1994; Wehrens et al., 2017). (c) Overview map of the recent Lake Grimsel area with the coring site (red point). (d) Catchment areas of Lake Grimsel before the damming of the lake in the year 1929 (green-black shaded; 2.8 km^2) and after the damming (green; 100 km^2). (Maps modified from *swisstopo.admin.ch; BA18064*)

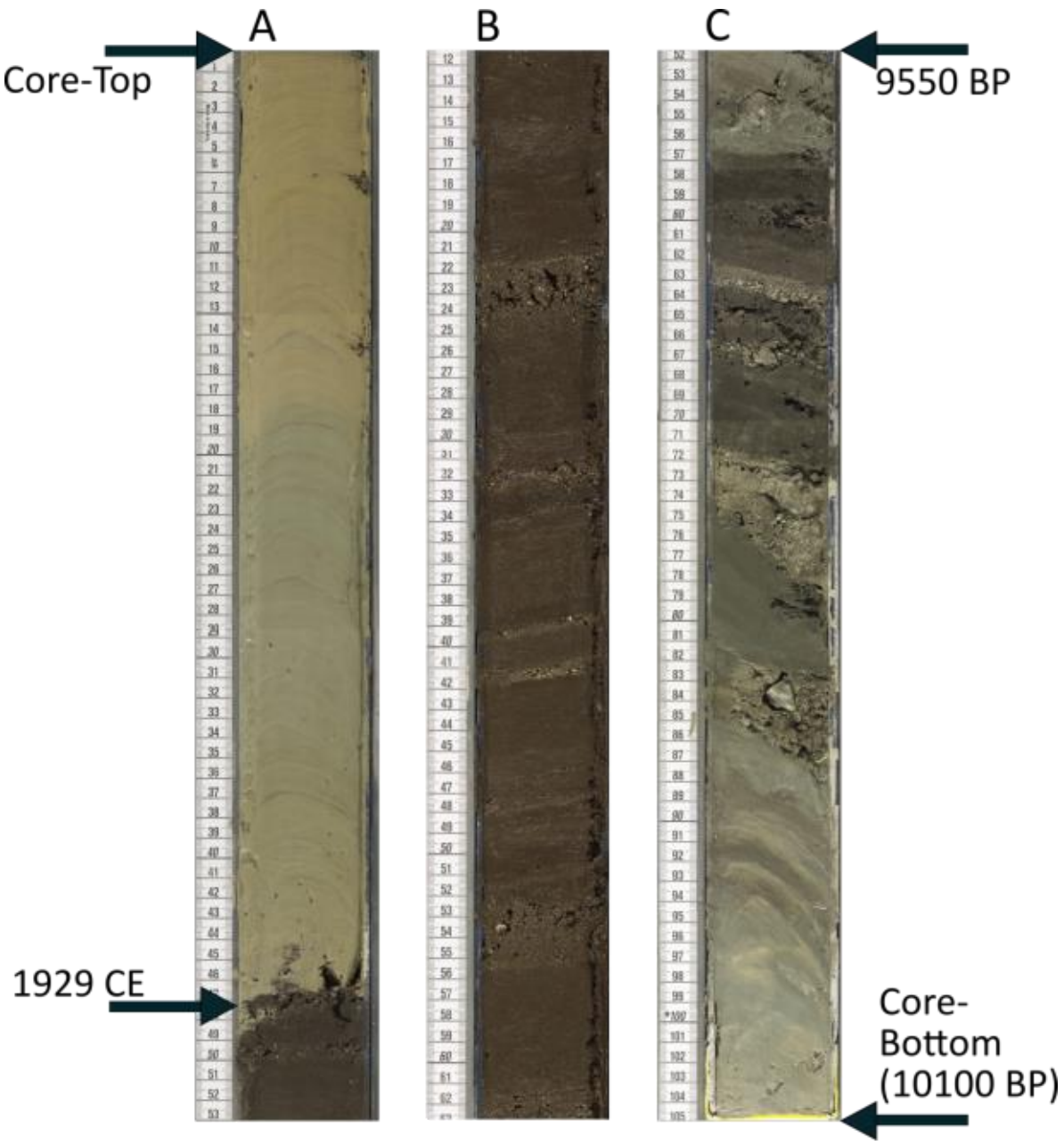

Figure 2: Photographs of the youngest (left), oldest (right) and average Holocene core sections. The oldest and deepest core section (right) is characterized by greyish clays at the beginning of sedimentation and clastic mass movement layers. Brownish colours are the result of first organic material accumulation. The presented section represents the first 300 years of sedimentation. The youngest core section (left) is characterized by a bright varved proglacial clay (Anselmetti et al., 2007). The lower part of the section is made out of brown gyttja which is the regular sediment type within the Holocene. The effect of the damming in the year 1929 is clearly visible as a sharp boundary between the dark gyttja layers and the bright clay. Beside the different in the brightness of the clays, the youngest and oldest clays are quite similar implying similar sedimentation processes.

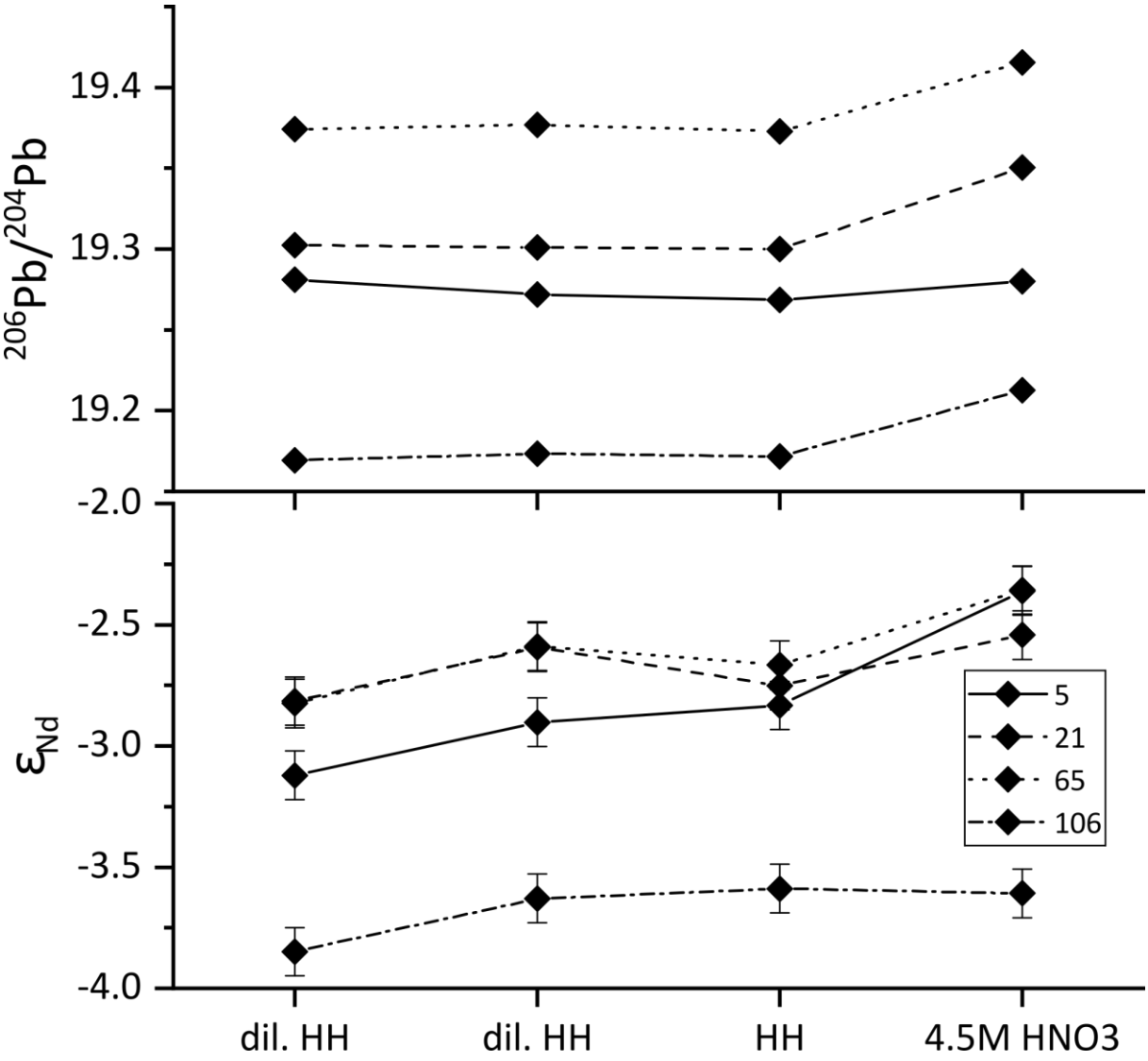

Figure 3: $^{206}Pb/^{204}Pb$ and Nd isotopic composition (expressed as ε_{Nd}) of four selected sediment samples during continuous leaching experiments. First and second leaching steps have been performed with the mild leaching solution of Blaser et al. (2016) (dil. HH) while in the third leaching step the solution of Gutjahr et al. (2007) (HH) were used. Isotopic variations are not noticeable during the first three leaching steps in the Pb isotopic composition with reductive leach solutions. Leaching with strong acids results in isotope excursions likely caused by partial dissolution of the detrital phase. The Nd isotopic composition changes continuous to radiogenic values during leaching. Isotopic compositions from the first reductive leaching step (most unradiogenic) are suggested to be closest to the original lake water signal.

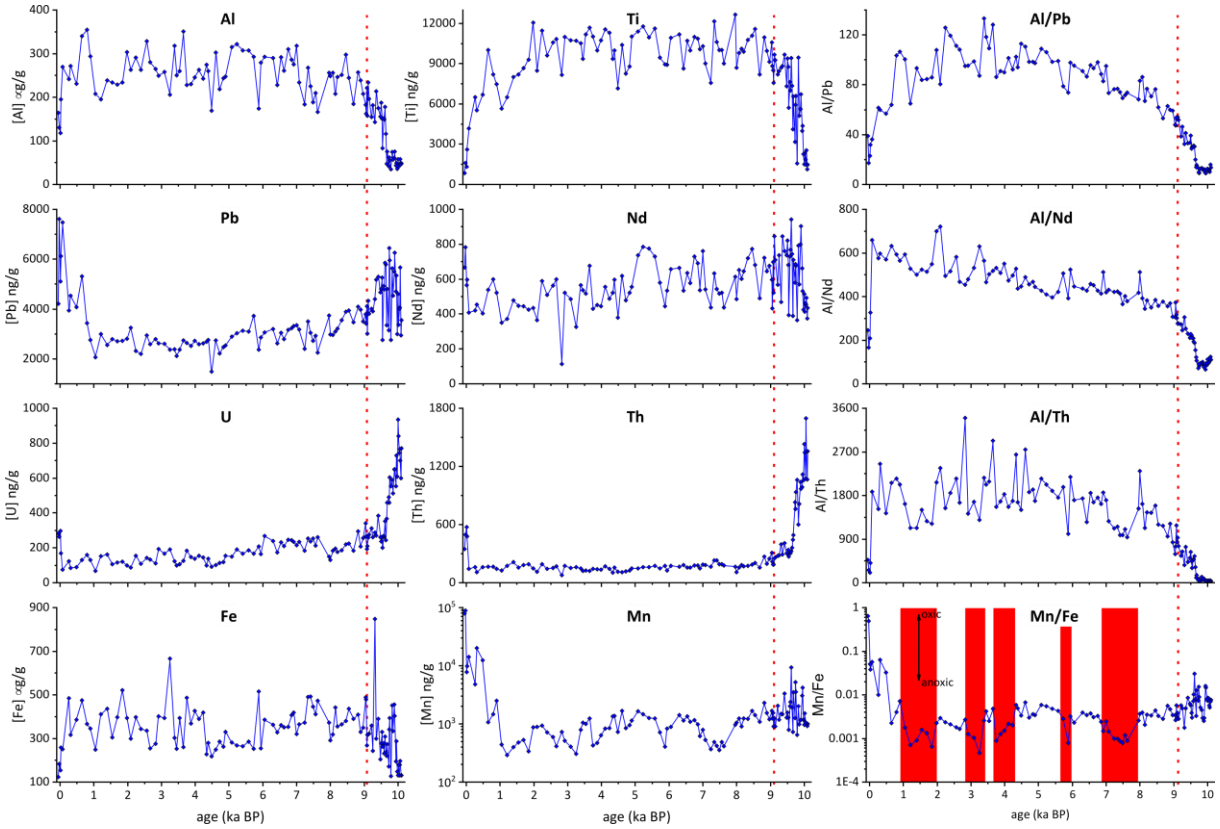

Figure 4: Selected element concentrations (Al, Ti, Pb, Nd, U, Th, Fe and Mn) shown in normalised concentrations (ng or µg per gram of leached sediment) and element ratios (Al/Pb, Al/Nd, Al/Th and Mn/Fe). The red dashed lines indicate the transition between the early deglacial and Holocene phase at 9 ka BP. The first deglacial phase is characterized by highly variable concentrations in all elements. Pb concentrations decrease during the Holocene with a strong increase in the latest 1000 years caused by atmospheric anthrogogenic Pb pollution. Mn/Fe ratio is strongly decreased during parts of the Holocene indicating ongoing anoxic bottom water conditions. Five phases (red boxes) can be identified with especially low Mn/Fe ratios. See text for discussion.

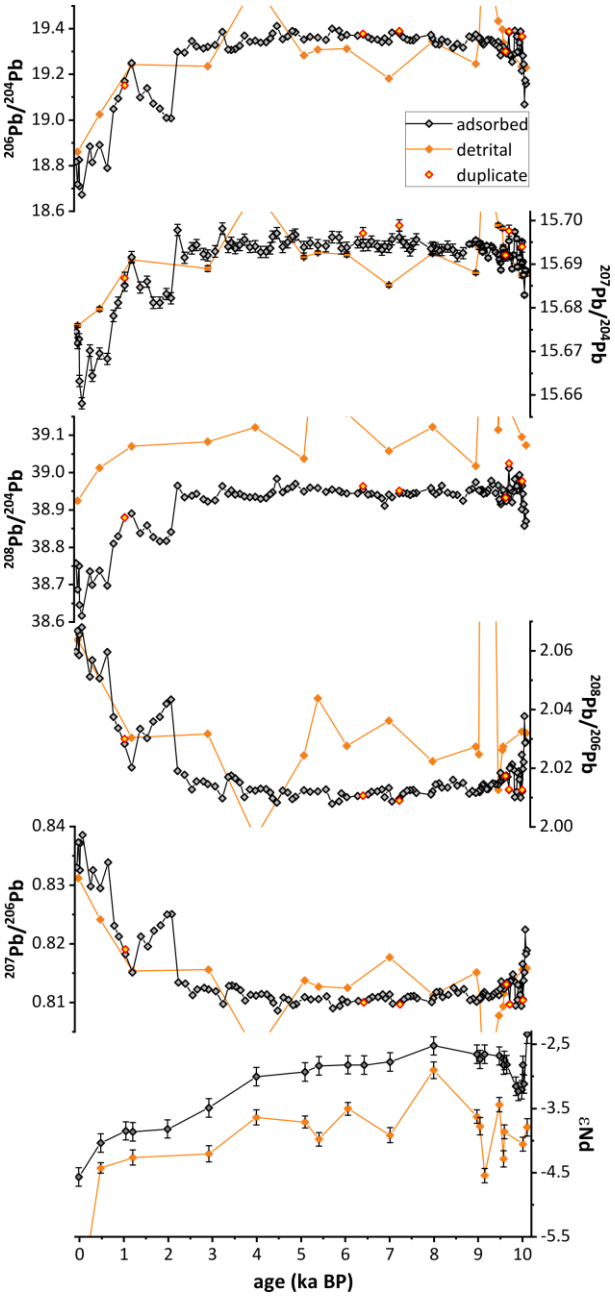

Figure 5: Holocene adsorbed (black) and detrital (orange) Pb ($^{206}Pb/^{204}Pb$, $^{207}Pb/^{204}Pb$ $^{208}Pb/^{204}Pb$, $^{207}Pb/^{206}Pb$ and $^{208}Pb/^{206}Pb$) and Nd isotopic records (expressed as ε_{Nd}) of Lake Grimsel. Yellow circles highlight duplicate samples. High variations in the detrital records results from the dissolution of a not representative mineral composition from the whole rock. For the sake of resolving fine-scale variations in the adsorbed Pb isotope records the y axes scales were chosen in a manner not to include the most extreme detrital compositions. The complete record can be found in Suppl. Fig. A5. The first initial deglacial phase shows a radiogenic excursion at the beginning and overall very variable Pb isotopic compositions. During the remainder of the Holocene all Pb isotope records are quite stable. ^{208}Pb is depleted in the adsorbed record relative to the detrital signal while $^{206}Pb/^{204}Pb$ and $^{207}Pb/^{204}Pb$ are comparable between the adsorbed and detrital phase. Pb isotopic excursions after 2.2 ka BP are controlled by anthropogenic Pb pollution. The Nd isotopic records are mainly characterized by a small radiogenic offset of the adsorbed signal compared to the detrital signal.

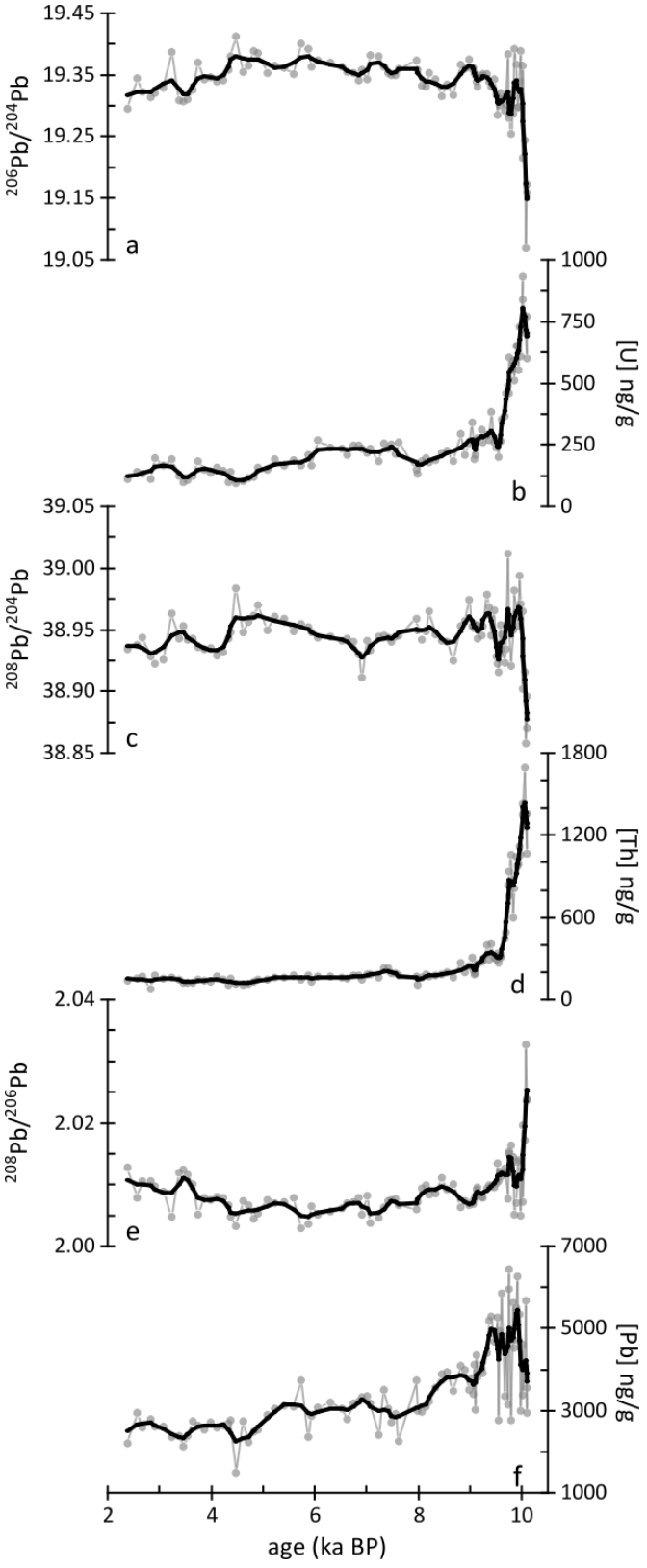

Figure 6: Selected Pb isotopic ratios plotted alongside the adsorbed normalised trace metal concentrations in Lake Grimsel sediments. Grey curves present individual results, while the thick black line show the smoothed evolution of each parameter. Smoothing carried out using a 1-2-3-2-1 weighting.

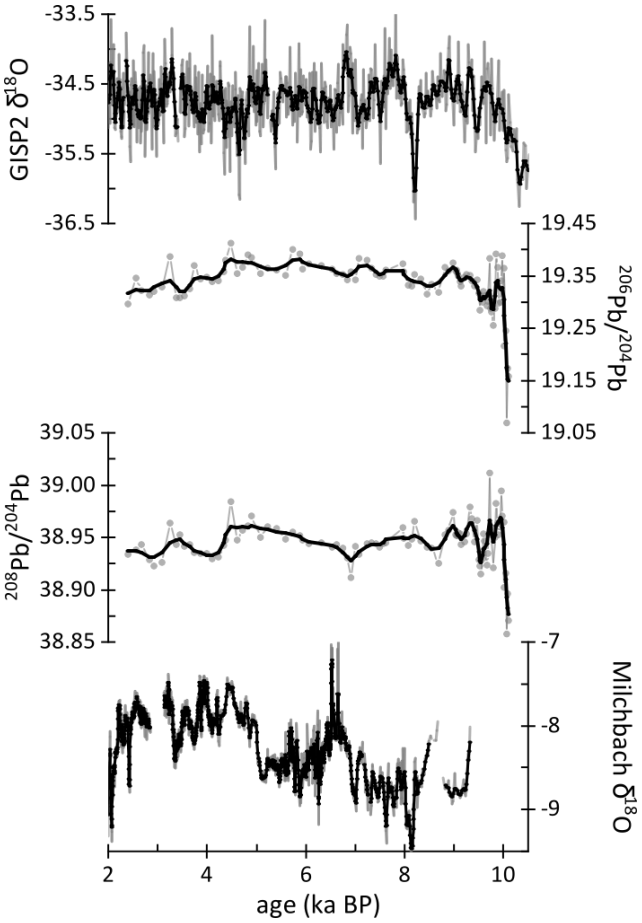

899

900 Figure 7: Comparison of the $^{206}Pb/^{204}Pb$ and $^{208}Pb/^{204}Pb$ ratios with the GISP2 $\delta^{18}O$ (Alley,
901 2004) and the Milchbach $\delta^{18}O$ speleothem record (Luetscher et al., 2011). The Lake Grimsel
902 Pb isotope records show no obvious correlation with climate perturbations recorded in either
903 Greenland ice or a nearby Alpine speleothem.

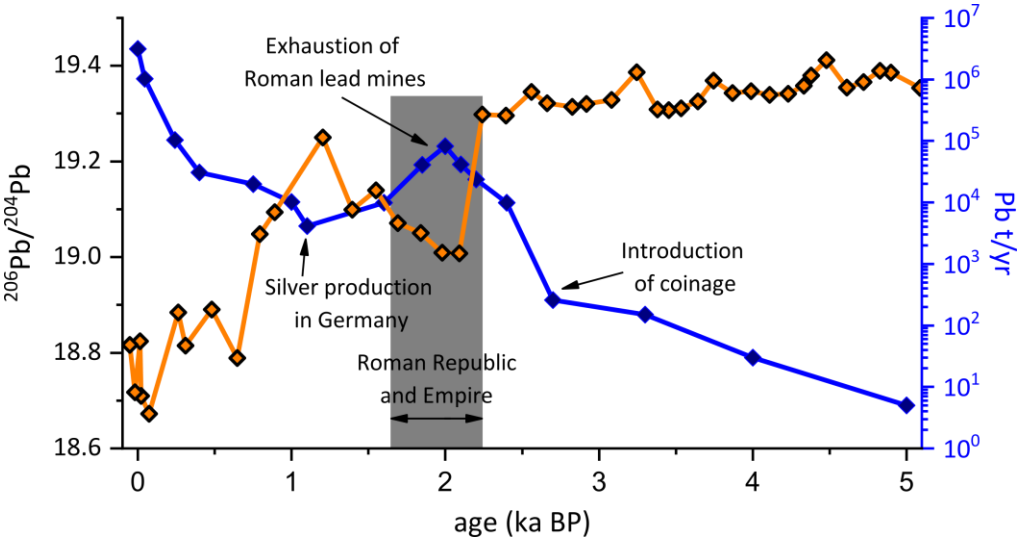

904

905 Figure 8: Adsorbed $^{206}Pb/^{204}Pb$ isotope record of the latest 5000 years compared to the world
906 wide lead production of the same interval (Settle and Patterson, 1980). A clear correlation
907 between the records after 2.2 ka BP is visible. The Pb isotope record strictly follows the mining
908 activity as well as the European cultural evolution (e.g. rise and fall of the Roman Empire
909 indicated as grey bar).